

ORIGINAL PAPER

Calmodulin is Required for Paraflagellar Rod Assembly and Flagellum-Cell Body Attachment in Trypanosomes

Michael L. Ginger^{a,1}, Peter W. Collingridge^b, Robert W.B. Brown^a, Rhona Sproat^b, Michael K. Shaw^b, and Keith Gull^b

^aFaculty of Health and Medicine, Division of Biomedical and Life Sciences, Lancaster University, Lancaster LA1 4YQ, UK

^bSir William Dunn School of Pathology, University of Oxford, South Parks Road, Oxford OX1 3RE, UK

Submitted November 18, 2012; Accepted May 9, 2013
Monitoring Editor: George B. Witman

In the flagellum of the African sleeping sickness parasite *Trypanosoma brucei* calmodulin (CaM) is found within the paraflagellar rod (PFR), an elaborate extra-axonemal structure, and the axoneme. In dissecting mechanisms of motility regulation we analysed CaM function using RNAi. Unexpectedly CaM depletion resulted in total and catastrophic failure in PFR assembly; even connections linking axoneme to PFR failed to form following CaM depletion. This provides an intriguing parallel with the role in the green alga *Chlamydomonas* of a CaM-related protein in docking outer-dynein arms to axoneme outer-doublet microtubules. Absence of CaM had no discernible effect on axoneme assembly, but the failure in PFR assembly was further compounded by loss of the normal linkage between PFR and axoneme to the flagellum attachment zone of the cell body. Thus, flagellum detachment was a secondary, time-dependent consequence of CaM RNAi, and coincided with the loss of normal trypomastigote morphology, thereby linking the presence of PFR architecture with maintenance of cell form, as well as cell motility. Finally, wider comparison between the flagellum detachment phenotypes of RNAi mutants for CaM and the FLA1 glycoprotein potentially provides new perspective into the function of the latter into establishing and maintaining flagellum-cell body attachment.

© 2013 Elsevier GmbH. All rights reserved.

Key words: Cell morphogenesis; flagellum assembly; flagellum function; paraflagellar rod *Trypanosoma brucei*; trypanosomatid.

Introduction

The paraflagellar rods in trypanosomatids and several other euglenozoan protists provide particularly elegant examples of extra-axonemal structures (Bastin et al. 1996; Portman and Gull 2010). As most recently revealed by cryo-electron tomography, the two major paraflagellar rod (PFR) proteins,

PFR1 and PFR2, assemble into a complex, ornate arrangement of filaments to form the rod's characteristic proximal, intermediate, and distal regions (Höög et al. 2012; Hughes et al. 2012; Koyfman et al. 2011). In the African sleeping sickness parasite *Trypanosoma brucei*, the PFR is attached to and runs alongside the axoneme from the point where the flagellum exits its flagellar pocket. The PFR serves a number of important functions, including critical roles in productive motility and normal cell swimming in *T. brucei* and related

¹Corresponding author;
e-mail m.ginger@lancaster.ac.uk (M.L. Ginger).

Leishmania parasites, respectively (Bastin et al. 1998; Maga et al. 1999). In African trypanosomes, the PFR acts as a platform into which enzymes with likely (Ginger et al. 2008; Pullen et al. 2004) or essential (Oberholzer et al. 2007) roles are assembled; orthologues of these enzymes are encoded within the nuclear genomes of the American trypanosome, *T. cruzi*, and *Leishmania*, too. Thus, the role of the PFR in motility may relate, in whole or in part, to its function in anchoring essential regulatory proteins. Yet, it is still not clear if the architecture of the PFR contributes an independent essential structural or bio-physical function to motility and how mechanistically such a function would be accommodated (see Höög et al. 2012; Hughes et al. 2012; Koyfman et al. 2011 for further recent discussion of these points). The possibility that the *T. brucei* PFR is physically connected to outer-dynein arms on outer-doublers 4, 5, and 6 (Hughes et al. 2012) is compatible with either regulatory or bio-physical roles for the PFR in motility.

A combination of proteomic approaches has revealed that the trypanosome PFR is likely to be composed of at least 30-40 different proteins (Portman et al. 2009), including PFR1, PFR2 and a number of proteins with motifs or domains that classically bind Ca^{2+} . This led to the suggestion that Ca^{2+} -dependent signalling cascades contribute to PFR function (Portman and Gull 2010; Portman et al. 2009), and is relevant since Ca^{2+} is a ubiquitous regulator of flagellar motility, including in trypanosomatids (Holwill and McGregor 1976). The inventory of putative PFR Ca^{2+} -binding proteins includes calmodulin (CaM), a small, classic EF-hand-containing protein that functions in many Ca^{2+} -dependent processes (Chin and Means 2000) and is found within several sub-structures of the axoneme in *Chlamydomonas reinhardtii* (DiPetrillo and Smith 2010; Dymek and Smith 2007; Smith 2002; Yang et al., 2001, 2004) and trypanosomes (Ridgley et al. 2000). However, a major immunologically accessible location determined by Ruben and co-workers for CaM in *T. brucei* is the PFR. Thus, CaM is an abundant PFR protein: it is found throughout the three characteristic domains of the PFR, as well as the connections that link (i) the PFR to the axoneme and (ii) the PFR to the flagellum attachment zone (FAZ) (Ridgley et al. 2000). Collectively, the phenotypes of various RNAi mutants (Broadhead et al. 2006; LaCount et al. 2002; Moreira-Leite et al. 2001; Sun et al. 2013; Vaughan 2010; Vaughan et al. 2008; Zhou et al. 2011) indicate attachment of the flagellum to the trypanosome cell body is essential for maintenance of trypomastigote morphology and, in many

instances, cell replication, too. In this work, we reveal the RNAi phenotype of CaM depletion in *T. brucei* is a total and catastrophic failure in PFR assembly. Elongation of an axoneme with no obvious ultrastructural defects still occurs following induction of CaM RNAi. However, the failure in PFR assembly is compounded by an apparent failure to secure the structural architecture of the flagellum through to the cytoplasmic face of the FAZ, and flagellum detachment occurs as a secondary consequence of calmodulin ablation by RNAi induction. Our data therefore point towards the importance of PFR assembly for maintenance of flagellum attachment to the cell body and identify another key role for the PFR in *T. brucei*. Moreover, our observations also perhaps help to explain why a residual PFR structure is retained along the proximal third of the flagellum in endosymbiont-bearing trypanosomatids, such as *Crithidia deanei* (Gadelha et al. 2005). The endosymbiont-bearing trypanosomatids swim with a fast-beating flagellum, but the function(s) of their relic PFR remain cryptic.

Results

CaM is Required for PFR Assembly

A bioinformatics search of the TriTrypDB resource (Aslett et al. 2010) reveals the existence of multiple isoforms of CaM encoded within the *T. brucei* nuclear genome. The CaM isoform targeted by RNAi in this work is encoded by a cluster of identical, tandem duplicated genes that code for a protein of 149 amino acids (Tb11.01.4621-Tb11.01.4624 in the TREU927 genome reference strain). Protein products encoded by this gene cluster were previously detected in the axoneme and PFR (Portman et al. 2009; Ridgley et al. 2000). The gene cluster is essential and deletion of one cluster from the diploid genome gave a haploid insufficiency phenotype of slow growth (Eid and Sollner-Webb 1991). Induction of CaM RNAi also resulted in a slowing of the growth rate (Fig. 1A) and cell motility was reduced, but the more striking effect of RNAi induction was a dramatic change in cell morphology (Figs 1B, 2, 3). Thus, early in the cell division cycle, before nuclear and kinetoplast S-phases have initiated, procyclic trypomastigotes normally possess a single flagellum which, except for the distal-tip, is attached to the cell body (Figs 2A, C, 3A). As early as 24 h post-induction of CaM RNAi, short cells possessing a single, free flagellum (i.e. not attached for much of its length to the cell body) began to

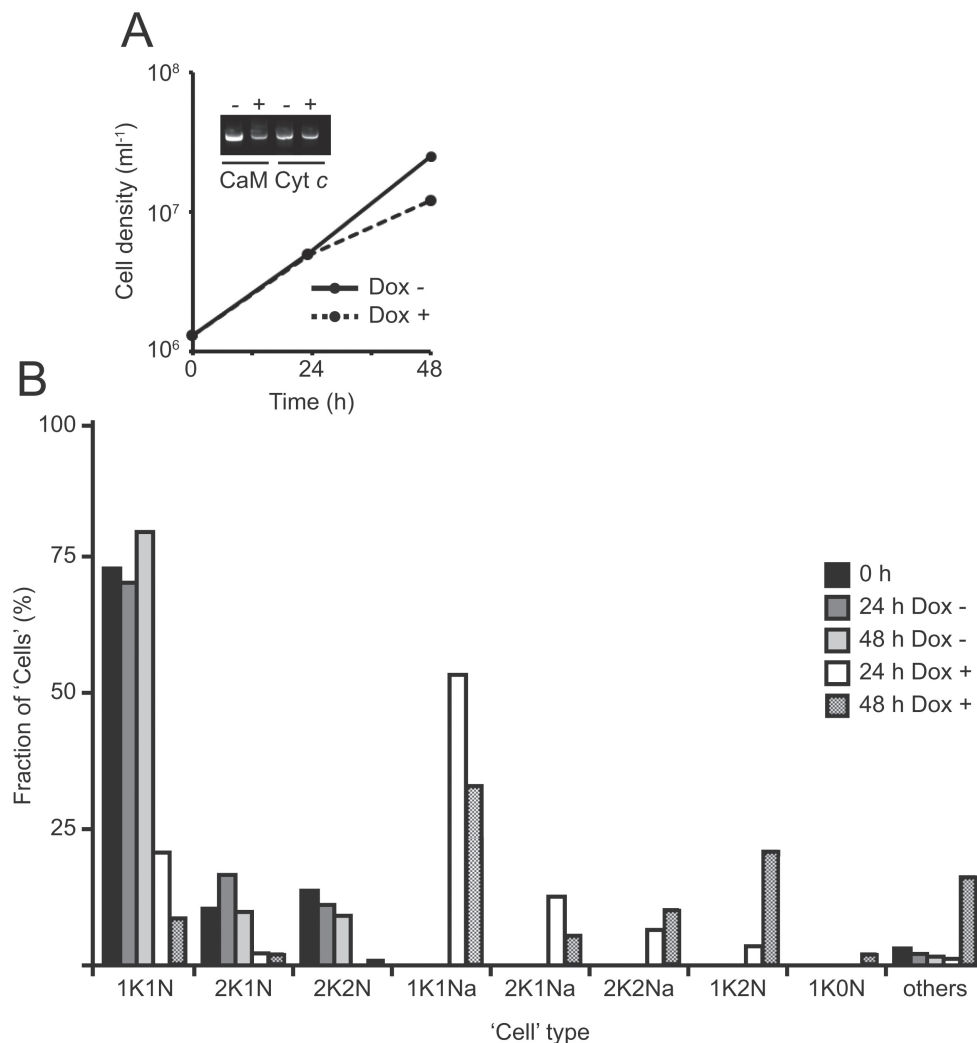


Figure 1. CaM is required for growth and normal cell morphology. **(A)** Growth of the CaM RNAi mutant. The inset shows the depletion of CaM mRNA as estimated using semi-quantitative reverse transcription-PCR after 16 cycles of PCR (see Methods) RNA was isolated 24 h after the induction of RNAi. Cytochrome *c* (Cyc *c*) was chosen as a control housekeeping mRNA for relative quantitation since CaM and cytochrome *c* are similarly sized proteins and the length of the mRNA can be expected to be similar. **(B)** Altered morphology of cells following induction of CaM RNAi. The number of nuclei and kinetoplasts (the structure containing mitochondrial DNA) per cell within the cultures counted for (A) were scored by epifluorescence microscopy after staining paraformaldehyde-fixed cells with 6-diamidino-2-phenylindole (DAPI). Segregation of newly replicated kinetoplasts is dependent upon basal body separation. The analysis revealed loss of normal 1K1N, 2K1N and 2K2N morphologies following RNAi induction and the appearance of abnormal (1K1Na, 2K1Na, 2K2Na) morphologies and multinucleate cell types (1K2N, others). Here 'abnormal' denotes flagellum detachment and/or loss of normal K-N positioning within cells; examples of normal trypanomastigote and CaM RNAi-induced morphologies are shown in Figures 2-3. For K-N counts, between 507 and 528 cells were scored at each time point. Data shown in this figure are representative of multiple RNAi induction experiments.

accumulate in the population (Fig. 3B). Similar-looking cells (Figs 2B, 3C) were also present by 48 h post-induction, alongside an increasing number of cells with two or more nuclei (categories "1K2N" and "others" in Fig. 1B). The appearance of multinucleate cells has been reported for

numerous RNAi mutants and, in part, reflects differences in cell cycle control check-points between trypanosomes and well-studied yeast and animal models (Ploubidou et al. 1999). Since cell phenotypes became progressively more abnormal after 48 h RNAi induction, we restricted further analysis

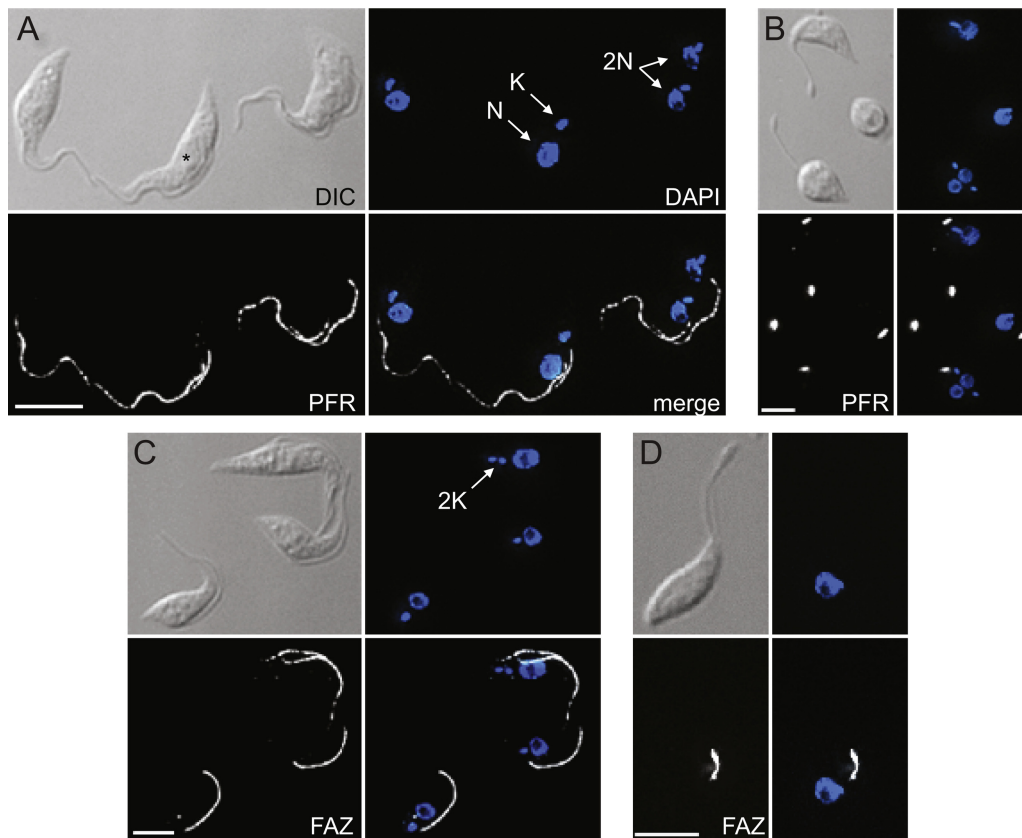


Figure 2. Loss of normal cell morphology and failures in PFR and FAZ assembly following CaM RNAi induction. **(A)** Non-induced CaM RNAi cells decorated for indirect immunofluorescence with the monoclonal antibody L8C4, which recognises PFR2. Fixed cells were stained for DNA using DAPI, and the image shows the PFR in three cells: a 1K1N cell possessing a single flagellum; at a later point in the cell cycle when a new flagellum is being assembled anterior to the old flagellum (asterisk in the DIC panel); in a mitotic 2K2N cell. **(B)** Cells induced for CaM RNAi for 42 h prior to fixation and indirect immunofluorescence with L8C4. **(C)** Non-induced CaM RNAi cells decorated for indirect immunofluorescence with the monoclonal antibody L3B2, which recognises a FAZ antigen. The FAZ signals in 1K1N and biflagellate 2K1N cells are shown. **(D)** A cell induced for CaM RNAi for 42 h prior to fixation and indirect immunofluorescence with L3B2. In cells with detached flagella, cytotactic cues imparted by flagellum and FAZ positioning are lost. Scale bars represent 5 μm .

of CaM RNAi mutants to early time-points to focus upon the normal-to-abnormal transition.

To look at the effect of CaM RNAi on flagellum ultrastructure we fixed whole cells and detergent-extracted cytoskeletons for TEM (Fig. 4). In a count of over 600 transverse flagellar sections from fixed whole cells, 82% of sections displayed some sort of obvious PFR abnormality¹. In ~80% of these

abnormal sections no PFR was seen (Fig. 4C, D); in the remaining sections there was massive accumulation of PFR-like electron dense material within the

¹ Data shown in Figure 1 come from an RNAi induction independent to those from which our EM analyses were made. The data in Figure 1 are also representative of multiple RNAi inductions. Thus from Figure 1A, the cell density at 48 h post-induction of RNAi is derived from approximately three doublings in cell number. Since flagella in African trypanosomes are not ephemeral – i.e. once assembled flagella from trypomastigote cells are not re-adsorbed at cell division or in response to

other cues – one could anticipate that at the point when cells were fixed for microscopy at least 12% of flagella present within the population of RNAi-induced cells would possess a normal-looking ‘axoneme-plus-PFR’ configuration (Fig. 4B). Moreover, the PFR (for which assembly lags behind axoneme extension; e.g. Pullen et al. 2004) would, to the point of RNAi induction, also be forming normally along the length of elongating flagella. Since greater than 80% of flagellar cross-sections show some form of PFR abnormality, this points to good penetration of the RNAi phenotype across the population of induced cells, even if RT-PCR estimate suggests only a 60-70% average reduction of CaM mRNA within individual cells. Combined, data from the TEM quantification and Figure 1 indicate a robustness for phenotype penetration between inductions (as noted in the earliest *T. brucei* inducible RNAi mutants; e.g. Wang et al. 2000).

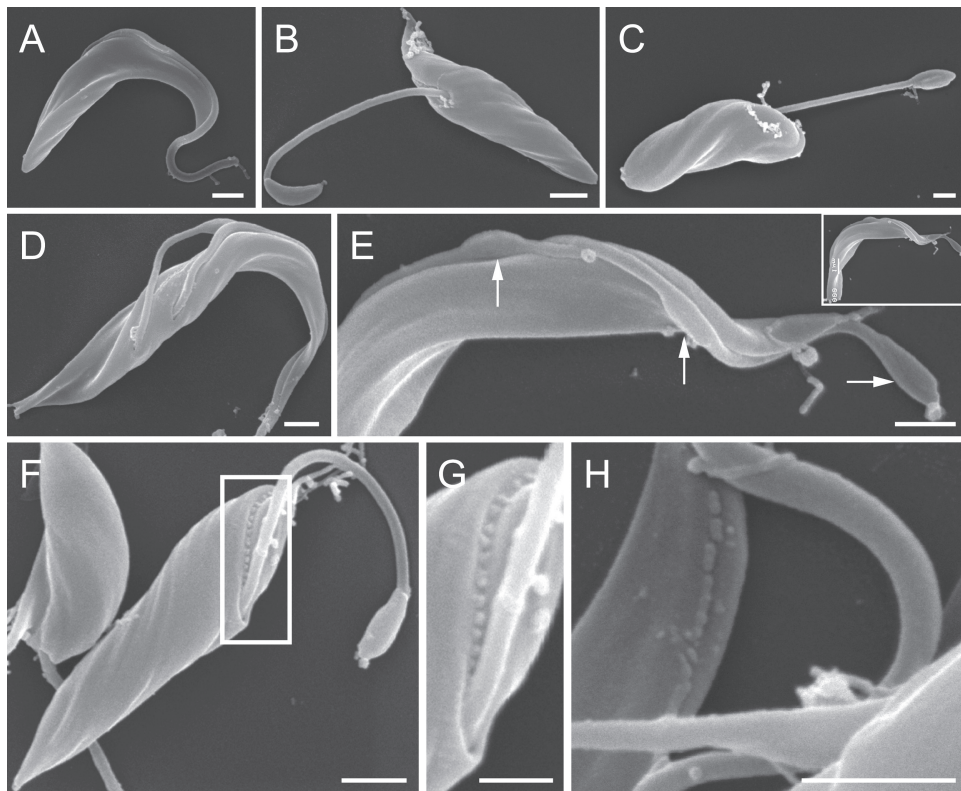


Figure 3. SEM: cell morphology in CaM RNAi-induced cells. (A) Typical procyclic trypomastigote morphology at an early point in the cell division cycle (i.e. 1 flagellum, 1K1N). (B–C) Short cells with a single, free flagellum are present at 24 h (B) and 48 h (C) post-induction of RNAi. (D) Flagellum detachment during elongation of the new flagellum. (E) Stable attachment of the new and the old flagella following RNAi induction. The entire cell is shown in the inset; ‘blobs’ (arrows) indicate how assembly of both flagella has been affected by RNAi (see main text). Images in (D) and (E) are of cells induced for CaM RNAi for 24 h. (F–G) Initial attachment of detached flagella is indicated by an indentation of the cell surface which contains bobbles of membrane and follows the left-handed helical pitch seen for an attached flagellum in a normal cell (the area shown at high magnification in G is boxed in F). (H) Where indentation of the plasma membrane was not obvious, membrane bobbles were often still present on the cell surface and marked a region of flagellum detachment (H). Scale bars represent 2 μ m, except (G) (500 nm).

flagellum (Fig. 4E). Importantly, the absence of a PFR was seen in both new and old flagella (Fig. 4C). Consistent with the accumulation in RNAi-induced cultures of cells with a free flagellum, a large number of the flagellar cross-sections observed by TEM were not attached to a cell body.

Often, PFR2 RNAi mutants (also known as ‘*snf*’ mutants) are referred to as lacking a PFR. However, there is a very significant difference between these published PFR2 RNAi mutants (Bastin et al. 1998, 2000; Broadhead et al. 2006; Pullen et al. 2004) and the CaM RNAi mutant described here: in PFR2 RNAi mutants the outer two zones of the PFR are not present whilst the innermost zone is still built (Bastin et al. 1998) attached to outer-doublet microtubules 4–7. In contrast, not even a rudimentary PFR is formed following CaM RNAi. To look further

at this failure in PFR assembly, we used detergent-extracted cytoskeletons fixed either in the presence or absence of tannic acid (to enhance contrast of microtubules and any microfilament-based structures attached to outer-doublet microtubules). In over 50% of cross-sections which contained an axoneme, but no PFR, we found no evidence that the supporting fibres (or struts) which attach the PFR to outer-doublet microtubules 4–7 were formed. In other cross-sections, electron density was associated with one (Fig. 4G), or less often 2–3 (Fig. 4H), outer-doublet microtubules of some cross-sections. This is distinct from the ultrastructural phenotype seen in the *PFR1/PFR2* null mutant of another trypanosomatid parasite *Leishmania mexicana*. In $\Delta PFR1/\Delta PFR2$ *L. mexicana* there is also no PFR formed, but in this mutant over

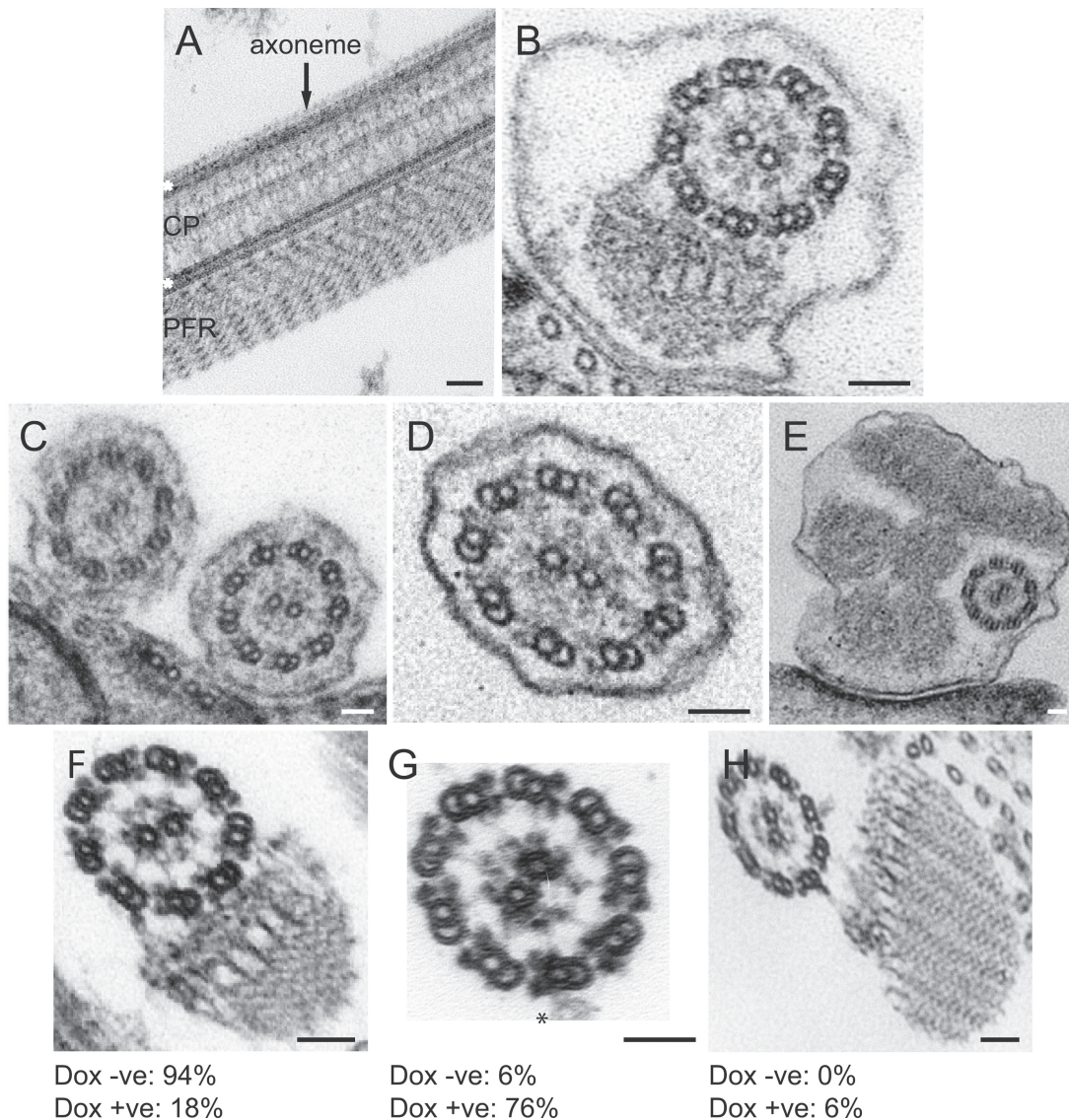


Figure 4. TEM: failure of PFR assembly in CaM RNAi mutants. (A) Longitudinal section of a detergent-extracted axoneme and its associated PFR from a cell not induced for CaM RNAi. The central pair (CP) microtubules of the axoneme and PFR are labelled, and the white asterisks denote outer-doublet microtubules. (B) Transverse cross-section of the wild type configuration of axoneme and PFR within an intact cell; only 18% (n=687) of transverse flagellum sections in fixed, CaM RNAi-induced cells showed this classic configuration. (C-D) Transverse sections through cells from CaM RNAi-induced cultures revealing flagella with an axoneme, but no PFR (60% of transverse sections). (E) Transverse section through a flagellum of a cell from a CaM RNAi-induced culture showing an axoneme surrounded by electron dense material that is “PFR-like” in appearance (22% of transverse sections). (F-H) Differences in flagellar architecture between RNAi induced and not induced states were quantitated in detergent-extracted cytoskeletons. In (G) the asterisk highlights an electron density which could correspond to one of the supporting fibres that attach the PFR to the axoneme, but similar electron densities were absent from > 50% of transverse sections and were rarely observed on multiple outer-doublet microtubules (the PFR is normally attached to outer-doublets 4-7). Samples were analysed after 48 h of RNAi induction. Scale bars represent 50 nm.

90% of flagellum cross-sections contain putative PFR attachment fibres to one or more outer-doublet microtubules (Maga et al. 1999). Thus, our analysis suggests CaM is essential for PFR-axoneme attachment fibre formation, and thence subsequent PFR assembly.

In PFR2 RNAi mutants a ‘blob’ is found at the distal end of the new flagellum (Bastin et al. 1999). This ‘blob’ contains PFR1 protein, as well as other minor PFR components; these proteins are moved to the flagellum distal tip by anterograde intraflagellar transport (IFT), but cannot be assembled to form a normal PFR due to the absence of PFR2 protein. Following cell division, the ‘blob’ is transported back to the cell body via a retrograde IFT pathway (Bastin et al. 1999). Immunofluorescence analysis using the monoclonal antibody L8C4, which recognizes PFR2, also confirmed the failure of PFR assembly in the CaM RNAi mutant, and indicated that ‘blob’-like structures seen by SEM (Fig. 3) contained major PFR proteins (Fig. 2B). In PFR2 RNAi mutants, the ‘blob’ is detergent-soluble and contains proteins that cannot assemble into a PFR in the absence of PFR2. In contrast, the immunofluorescence signal from the ‘blob’ in CaM RNAi mutants was retained in detergent-extracted cytoskeletons (data not shown). Since RNAi yields reduction in the abundance of the targeted mRNA, rather than a total ablation, the retention of the blob in cytoskeletons presumably occurred because a reduced amount of CaM produced following RNAi induction was still sufficient to occasionally build one or more attachment fibre at points along the length of the axoneme, and at these points PFR2, and potentially other PFR components, then accumulated. Judging from immunofluorescence images, the points along the axoneme where PFR attachment fibres could form were commonly at the distal tip and at the exit point from the flagellar pocket (where normally in *T. brucei* the PFR is first formed). The analysis by TEM revealed the accumulation of PFR proteins could start to take on a paracrystalline arrangement, albeit generally lacking the ornate form seen in the PFR built by wild-type *T. brucei* (Figs 4E, H, 5B).

Loss of Flagellum-cell Body Attachment in CaM RNAi Mutants

The presence of a detached, free flagellum was a notable characteristic in many CaM RNAi cells (Fig. 3B, C), and in some biflagellate cells detachment evidently occurred during elongation of a new flagellum (Fig. 3D). However, we also observed cells fixed at either 24 h or 48 h post-RNAi

induction in which new and old flagella were both clearly attached to the cell body (Fig. 3E). The transverse-section shown in Figure 4C is taken through a biflagellate cell in which both new and old flagella lack a PFR, but both flagella are attached to the cell body. Importantly, cells such as those shown in Figure 3E and Figure 4C suggest attachment must initially be the default status for many flagella built following induction of CaM RNAi. Moreover, a careful view of CaM RNAi mutants by light microscopy indicated that in short cells with an apparently free flagellum, cell body attachment was evident at the proximal end of the flagellum. Indirect immunofluorescence with the monoclonal antibody L3B2, which recognises the FAZ filament protein FAZ1 (Vaughan et al. 2008) indicated that on the cytoplasmic face of the plasma membrane a short FAZ (of some description) underlay the region of flagellum-cell body attachment (Fig. 2D). Flagellum detachment is therefore a time-dependent phenomenon.

SEM of cells with a detached flagellum also provided a different slant on the initial attachment between the flagellum and the cell body. The cell in Figure 3F, for instance, displays an indentation or ‘canal’ on the cell surface which extends from the flagellar pocket with a left-handed helical pitch (shown at higher magnification in Fig. 3G) similar to that adopted by the elongating new flagellum (Moreira-Leite et al. 2001). Similar canals were evident in other cells with a detached flagellum and, like the example shown in Figure 3F, evenly spaced bobbles of membrane often sat within the flagellar canal. Alternatively, even when a flagellar canal was not evident on the cell surface, evenly spaced membrane bobbles could still be seen underlying the region where the flagellum had presumably detached from the cell body (Fig. 3H). The presence of these membrane bobbles has an obvious parallel with the flagellar membrane or ‘sleeve’ that is extended by the flagella connector even in the absence of axoneme formation (Davidge et al. 2006). However, our observation of the bobbles contrasts with the mode of flagellum detachment seen in FLA1 RNAi cells; in these mutants, as a consequence of RNAi against a *T. brucei* homolog of the *T. cruzi* surface glycoprotein gp72, the newly extending flagellum is never attached to the cell body (Moreira-Leite et al. 2001). We reported in an earlier publication that when viewed at high magnification the cell surface of this RNAi mutant remains smooth (Davidge et al. 2006). Some thin section micrographs of the CaM RNAi mutant also suggested that during detachment flagella leave behind a bobble of flagellar membrane on the cell surface

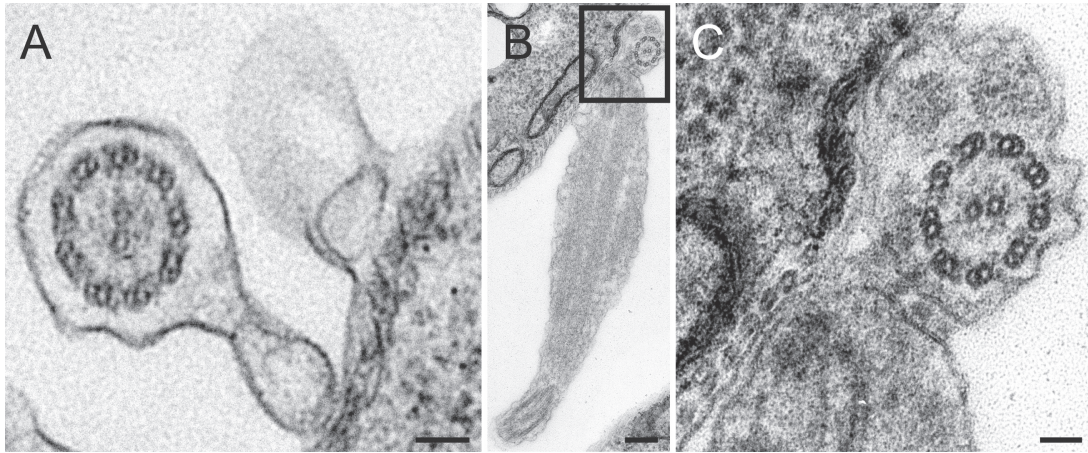


Figure 5. Flagellum detachment and the flagella connector formation in CaM RNAi mutants. **(A)** Transverse section of a PFR-minus flagellum likely to be in the process of detaching from the cell body; detachment should leave a bobble of flagellar membrane on the cell surface. **(B-C)** Despite accumulation of large amounts of PFR proteins at the flagellar distal tip, the flagella connector which is formed between new and old flagella before the new flagellum exits the flagellar pocket is able to persist in CaM RNAi mutants. The area shown at high magnification in (C) is boxed in (B). Images taken at 48 h post-induction of RNAi. Scale bars represent 50 nm (A and C) or 250 nm (B).

(Fig. 5A). Finally, images of the flagella connector, which connects the tip of the elongating new flagellum to the side of the old flagellum, suggest that this cytoskeletal structure is still built and then retained between new and old flagella even though both have extreme abnormalities caused by CaM depletion (Fig. 5B, C).

Discussion

In trypanosomes, inducible RNAi provides a tractable system for understanding how depletion of essential gene products leads to cell death. Here, our studies reveal how RNAi depletion of a trypanosome CaM produces an early, dramatic effect on construction of the PFR, followed at later time-points by the loss of flagellum-cell body attachment and the loss of normal trypanomastigote morphology. CaM is classically considered a multi-functional protein within cells, binding in Ca^{2+} -dependent fashion to numerous target proteins, although there are several, as yet unstudied, genes annotated as 'putative CaM' in the *T. brucei* genome. For the isoform analysed by RNAi in this work (encoded by gene cluster Tb11.01.4621-Tb11.01.4624) indirect immunofluorescence using specific, affinity-purified antibodies raised against native CaM protein detected antigen(s) within the PFR, axoneme, and at only a few vacuolar sites within the cell body (Ridgley et al. 2000). Those immunofluorescence signals from the cell body

provide the sole, and therefore equivocal, evidence that the CaM isoform studied here is present at an intracellular location other than the flagellum. Significantly, CaM was not detected at the cytoplasmic face of the FAZ in the study by Ridgley et al. (2000). Plausibly, we have studied the function a flagellum-specific isoform of CaM. Moreover, whilst we cannot formally exclude the possibility that loss of normal cell morphology and/or the appearance of multi-nucleate monsters is a consequence of CaM depletion from sites within the cell body, the phenotypes of flagellum detachment and the degeneration of trypanomastigote morphology discussed below are both readily explained as a consequence of the primary, complete failure in PFR assembly.

Aside from the major proteins PFR1 and PFR2, the kinesin-9 family protein KIF9B is the only other structural protein of the flagellum that we know to be essential for construction of a PFR (Demonchy et al. 2009). This protein is reported to be present in the flagellar basal body and the axoneme, but not the PFR. Although in possession of a characteristic N-terminal kinesin motor domain, it is not known whether KIF9B actually exhibits microtubule motor function. Indeed, how KIF9B serves its essential role in PFR construction or function is not yet clear although several suggestions have been put forward (Demonchy et al. 2009). Protein-protein interaction networks have also been mapped for several other PFR proteins, but none of these components, thus far, appear to

be individually necessary for motility or PFR construction (Lacomble et al. 2009a; Portman et al. 2009; Pullen et al. 2004). The primary effect of CaM RNAi appears to be that the structures attaching the PFR to the axoneme (through doublet microtubules 4-7) are not built. The deployment of CaM to attach a significant architectural feature to outer-doublet microtubules provides an intriguing parallel with a related EF-hand containing protein from *C. reinhardtii*, DC3, which is required for efficient placement of outer-arm dyneins into the outer-dynein arm docking complexes (Casey et al. 2003). There are, however, some sites along axonemes in CaM RNAi-induced mutants where PFR-axoneme linkages are built (presumably at sites where sufficient CaM can be incorporated), but here the main domain structure of the PFR is still abnormal and the highly organized three domain structure is not constructed properly. This may be a simple dependency upon the primary failure, but it is also suggestive of a role for CaM in at least two PFR construction phases, and is perhaps reflected in the incorporation of CaM into distal, proximal and intermediate PFR domains in wild type cells (Ridgley et al. 2000).

CaM RNAi and Cell Motility

Motility in our CaM RNAi mutant was defective. Absence of a PFR provides an obvious explanation for the motility phenotype, but even though axonemes exhibited a '9+2' configuration with intact-looking dynein arms, radial spokes, and central pair (CP) in TEM cross-sections we did not examine the motility defect in depth for two reasons: (i) localisation studies by Ridgley et al. (2000) indicated the presence of CaM in the radial spokes and CP, as well as PFR – if the CaM isoform we targeted by RNAi is indeed present in axoneme sub-structures, as well as the PFR, motility is potentially compromised as result of CaM loss from the axoneme, as well as from the failure in PFR assembly; (ii) analysis of the *L. mexicana* $\Delta PFR1/\Delta PFR2$ mutant means the role for a PFR as a structure *per se* in flagellum beating has already been considered. Moreover, the *Leishmania* study utilised a mutant background where axoneme ultrastructure is more likely (than our CaM RNAi mutant) to be unaffected and utilised a trypanosomatid species where the flagellum is naturally free from, rather than attached to, the cell body (Maga et al. 1999).

PFR Function and Cell Morphogenesis

Assembly of a normal-looking PFR is essential for cell motility of *T. brucei* and promastigote form

Leishmania (Bastin et al. 1998; Lye et al. 2010; Maga et al. 1999; Santrich et al. 1997). In bloodstream *T. brucei* proper assembly of the PFR is essential for cell division, too (Broadhead et al. 2006; Griffiths et al. 2007). There is also a suggestion (Ralston et al. 2006) that the motility function provided by the PFR is essential for cytokinesis of procyclic (or tsetse midgut form) *T. brucei* (the same lifecycle stage as that used in the experiments reported here). Thus, a number of procyclic *T. brucei* RNAi mutants have been described where expression of either PFR1 or PFR2, the two major PFR proteins, was silenced (Bastin et al. 1998, 1999, 2000; Broadhead et al. 2006; Poon et al. 2012; Ralston et al. 2006; Rusconi et al. 2005). In these mutants a rudimentary PFR resembling the proximal domain of a normal PFR remained (Bastin et al. 1998, 1999; Broadhead et al. 2006), but the flagellum did not properly propagate waveforms from the flagellum distal tip to the base. Instead, the flagellum rapidly switched between attempting the principal waveform and wave reversal (Branche et al. 2006). As a consequence, cells exhibited no net forward motility, but in a PFR2 mutant described by Ralston et al. (2006) cell rotation was also compromised as a result of flagellum paralysis. Loss of cellular rotation was proposed as the explanation for a failure of cytokinesis in the PFR2 RNAi mutant generated by Ralston and co-workers, and perhaps pointed towards an essential role for PFR-dependent motility in cytokinesis as the reason why Hunger-Glaser and Seebeck (1997) had been unable to create *PFR2* gene deletion mutants in *T. brucei* some years previously. In their experiments, Hunger-Glaser and Seebeck were able to delete one locus of tandemly arranged *PFR2* genes from diploid procyclic *T. brucei* but failed in attempts to delete the remaining gene array. However, although the data from Ralston et al. (2006) are compelling, the work is also somewhat contentious because for several years previously, and in different strain backgrounds (Poon et al. 2012), the paralysis of PFR1 and PFR2 RNAi mutants (also commonly known as *snl*-mutants) had been reported to have little or no effect on cell division and growth in procyclic cells, and to only be lethal in bloodstream forms (Bastin et al. 1998, 1999, 2000; Broadhead et al. 2006; Poon et al. 2012; Rusconi et al. 2005). The CaM RNAi phenotype offers an alternative insight into essential function(s) of a PFR in cell morphogenesis.

In the absence of even a rudimentary PFR, stable connectivity between the structural architecture of the flagellum (i.e. the axoneme in our CaM RNAi mutant) and the cytoplasmic face of the FAZ is not

maintained. Thus, in CaM RNAi cells the elongating new flagellum, attached at its distal tip to the old flagellum by the flagella connector, can be found in close association with the cell body. Yet, proteins such as FLA1, which is absolutely essential for flagellum-cell body attachment (Moreira-Leite et al. 2001; see also below), and other FAZ components are unable to maintain flagellum-cell body attachment if the structural connections normally made from a PFR to the FAZ do not assemble. In that regard, it is relevant to note that from published immuno-gold microscopy CaM is present within the attachment fibres that extend from the PFR down to the flagellar membrane face of the FAZ (Ridgley et al. 2000). With the possible apparent exception of a recently described FLA1BP² RNAi mutant (Sun et al. 2013), studies with various RNAi mutants have shown flagellum detachment in *T. brucei* typically has a severe effect on cell morphogenesis (Broadhead et al. 2006; LaCount et al. 2002; Moreira-Leite et al. 2001; Vaughan 2010; Zhou et al. 2011): the old flagellum provides cytotactic cues to position the elongating new flagellum and FAZ, thereby defining a pattern that influences the overall helical arrangement of the cytoskeleton (Moreira-Leite et al. 2001). Crucially, FAZ positioning is believed to impart important directional cues for cleavage furrow ingression during cytokinesis (Robinson et al. 1995). Upon re-entry into a new cell cycle, cytotactic cues for flagellum elongation and FAZ assembly are absent from cells with detached flagella, and cell morphogenesis subsequently fails completely. Such failures in morphogenesis can incorporate a variety of phenotypes including the accumulation of multinucleate cells (e.g. LaCount et al. 2002; Moreira-Leite 2002). For the CaM RNAi mutant morphological diversity included the appearance of short cells, which conceivably relates to elongation of short FAZ, and an increase in multinucleate cells. Thus to summarise: (i) in addition to an essential function in motility, a PFR is required for robust attachment of the flagellum to the trypanosome cell body and thence cell morphogenesis; (ii) PFR-dependency in sustaining attachment of the flagellum to the cell body therefore provides an explanation for why Seebeck and co-workers failed in their attempts to delete all copies of the *PFR2* gene from procyclic *T. brucei* (Hunger-Glaser and Seebeck 1997).

Intriguingly, natural variations of PFR structure are found in non-pathogenic trypanosomatid species which host a bacterial endosymbiont within

the cytosol (e.g. *Crithidia deanei*) and possess a free flagellum. *C. deanei* lacks *PFR2* gene copies and builds a much-reduced structure that extends only a third of the way along the mature flagellum (Gadelha et al. 2005). This reduced PFR also forms before the flagellum exits the flagellar pocket. PFR function in *C. deanei* and the other endosymbiont-containing trypanosomatids is cryptic, although the possibility that a reduced PFR might facilitate attachment to the epithelial lining of the digestive tract in the parasite's insect vector has been put forward (Gadelha et al. 2005). Unlike the irregular waveforms and reduced beat frequencies of PFR-minus *L. mexicana* (Maga et al. 1999; Santrich et al. 1997;), the waveform, beat frequencies, and swimming speed of *C. deanei* are comparable to fast-moving trypanosomatid species which possess a PFR (Gadelha et al. 2007). Orthologues of FAZ proteins characterised to date in *T. brucei* are present in the genomes of trypanosomatids that assemble flagella which are free of the cell body. Thus, in view of CaM RNAi phenotype described here, we suggest that another likely function of the highly-reduced PFR in the fast-swimming *C. deanei* is to help facilitate flagellum-cell body attachment as this organism's free flagellum emerges from the flagellar pocket exit point.

CaM RNAi and FLA1 Function

FLA1 is a *T. brucei* homolog of the *T. cruzi* glycoprotein gp72; it is concentrated along the flagellum and within the flagellar pocket of procyclic and bloodstream form *T. brucei* (Nozaki et al. 1996). In the absence of FLA1 the flagellum does not attach to the cell body (LaCount et al. 2002; Moreira-Leite et al. 2001). Although function(s) of the glycan moieties on FLA1 have not yet been determined, carbohydrate-carbohydrate or carbohydrate-lectin interactions between molecules of flagellar and plasma membranes are ideal for contributing to an adhesion mechanism which must be fluid enough to support vigorous flagellar beating. Indeed, the flagellum detachment phenotype evident in procyclic mutants defective for GDP-fucose biosynthesis is readily explained by perturbation of glycan architecture in surface-exposed molecules (Turnock et al. 2007). Since absence of FLA1 results in elongation of a flagellum that is never attached along its length to the cell body, FLA1 is clearly established as a critical, if not master, regulator of the initial flagellum-cell body attachment. However, we have discovered here that FLA1 and other FAZ components (e.g. FAZ1; Vaughan et al. 2008; FLA1BP; Sun et al. 2013) are insufficient

² FLA1BP, FLA1-binding protein.

to maintain flagellum-cell body adhesion of even motility-defective flagella, if the PFR cannot connect the structural architecture of the flagellum to the FAZ. Just as it is conceivable that FLA1 is a component of recently described 'staples' that connect the flagellum to the cell body (Höög et al. 2012) and/or the better known maculae adherens plaques, which are also formed between the flagellar and plasma membranes (Sherwin and Gull 1989; Vickerman 1969), it is possible that the regularly spaced membrane bobbles left within the flagellar canal following flagellum detachment in the CaM RNAi mutant denote the position of either FAZ staples or maculae adherens plaques.

Methods

Cell culture and RNAi: Procyclic *T. brucei* (cell line 29-13; Wirtz et al. 1999) was cultured in SDM-79 medium containing 10% v/v heat-inactivated foetal bovine serum, as described previously (Brun and Schönenberger 1979). The 29-13 cell line is genetically modified to express a tet-repressor protein and T7 RNA polymerase, meaning these cells are amenable to inducible RNAi. For RNAi the primer combination 5'-aatggatccaactcctcgttagttgattggc-3' and 5'-gccaagcttaactctccaacgacagatc-3' (BamHI and HindIII sites underlined and in italics, respectively) was used to amplify a partial open-reading frame from the CaM gene cluster encoded by Tb11.01.4622 – Tb11.01.4624. The resultant PCR amplicon was digested with BamHI and HindIII and sub-cloned into p2T7-177 RNAi plasmid (Wickstead et al. 2002) that also been BamHI-HindIII-digested. Procyclic *T. brucei* was transfected with the p2T7-177-CaM RNAi construct and stable transformants selected using phleomycin (3 µg ml⁻¹) according to standard methods (McCulloch et al. 2004). RNAi was induced by addition of doxycycline to a final concentration of 1 µg ml⁻¹; cell counts were made using a Neubauer haemocytometer and cells were maintained free of selectable agents (phleomycin, hygromycin and G418) for 48 h prior to the start of RNAi-induction. RNA was extracted from cultures using a GeneJet RNA Isolation Kit (Fermentas) and cDNA synthesised from 3 µg total RNA using a Maxima First Strand cDNA Synthesis Kit (Fermentas). In PCR, 1 µl aliquots of cDNA were used directly as template in reactions that also contained of forward primer and reverse primer. PCR reactions were set up using DreamTaq Green PCR Master Mix (Fermentas); annealing temperature for primers was 52 °C, the extension time for Taq polymerase was 60 sec, and progress of the reaction was checked every two cycles from cycle 12 onwards. The forward primer (5'-cgctattattagaacagtttctgtac-3') corresponded to sequence from the spliced leader RNA that is *trans*-spliced to all mRNA species in trypanosomes. The reverse primer corresponded to sequence from the 3' untranslated region of either CaM (5'-acataaacgaaggaagc-3') or cytochrome *c* (5'-ttctctctccatcctctgc-3') genes. Cytochrome *c* was chosen to estimate relative changes in CaM expression following RNAi induction because it is a housekeeping gene of similar length to CaM.

Microscopy: For transmission electron microscopy (TEM), whole cells were initially fixed by addition of 1 ml 25% v/v glutaraldehyde to 9 ml of culture at ambient temperature. After

5 min fixation cell pellets were collected by centrifugation (500 x *g*, 3 min), transferred into a buffered fixative (2.5% glutaraldehyde, 2% paraformaldehyde, 0.1% picric acid in 100 mM phosphate, pH 7.0), pelleted in an Eppendorf tube, and the fixation continued for 2-24 h at 4 °C. Samples were post-fixed in 1% osmium in 100 mM phosphate (pH 7.0) for 1.5 h in the dark at 4 °C, dehydrated, and embedded in epoxy resin. Cytoskeletons were prepared for electron microscopy by washing cells in 1% NP-40 in PEME before fixing samples and embedding in resin as above. Ultrathin (~70 nm thick) sections were double stained with uranyl acetate and lead citrate and examined in a FEI Tecnai 12 electron microscope. Cells were prepared for scanning electron microscopy (SEM) as described previously (Davidge et al. 2006; Moreira-Leite et al. 2001). For light microscopy, cells were settled onto glass slides and either fixed directly with paraformaldehyde (3.7% w/v in PBS) or extracted for 0.5 min with PEME containing 1% v/v NP-40 prior to fixation. Fixed preparations were decorated for immunofluorescence with the monoclonal antibodies L8C4 and L3B2 as described previously (Kohl et al., 1999), and cells were imaged at 60x magnification using an Applied Precision DeltaVision Microscope and a Roper Scientific Photometrics Cool SNAP HQ camera.

Acknowledgements

This work was supported by a Royal Society University Research Fellowship (to MLG) and The Wellcome Trust (to KG). PWC was supported by a studentship from BBSRC and RWBB by a Lancaster University Studentship. Support for the microscopes used in this work came from the BBSRC (BBF0109311) and the EP Abraham Trust.

References

- Aslett M, Aurrecochea C, Berriman M, Brestelli J, Brunk BP, Carrington M, Depledge DP, Fischer S, Gajria B, Gao X, Gardner MJ, Gingle A, Grant G, Harb OS, Heiges M, Hertz-Fowler C, Houston R, Innamorato F, Iodice J, Kissinger JC, Kraemer E, Li W, Logan FJ, Miller JA, Mitra S, Myler PJ, Nayak V, Pennington C, Phan I, Pinney DF, Ramasamy G, Rogers MB, Roos DS, Ross C, Sivam D, Smith DF, Srinivasamoorthy G, Stoeckert CJ Jr, Subramanian S, Thibodeau R, Tivey A, Treatman C, Velarde G, Wang H (2010) TriTrypDB: a functional genomic resource for the Trypanosomatidae. *Nucleic Acids Res* **38**:D457–D462
- Bastin P, Matthews KR, Gull K (1996) The paraflagellar rod of Kinetoplastida: solved and unsolved questions. *Parasitol Today* **12**:302–307
- Bastin P, Sherwin T, Gull K (1998) Paraflagellar rod is vital for trypanosome motility. *Nature* **391**:548
- Bastin P, Ellis K, Kohl L, Gull K (2000) Flagellum ontogeny in trypanosomes studied via an inherited and regulated RNA interference system. *J Cell Sci* **113**:3321–3328
- Bastin P, Pullen TJ, Sherwin T, Gull K (1999) Protein transport and flagellum assembly dynamics revealed by analysis of the paralysed trypanosome mutant *snl-1*. *J Cell Sci* **112**:3769–3777

- Branche C, Kohl L, Toutirais G, Buisson J, Cosson J, Bastin P** (2006) Conserved and specific functions of axoneme components in trypanosome motility. *J Cell Sci* **119**:3443–3455
- Broadhead R, Dawe HR, Farr H, Griffiths S, Hart SR, Portman N, Shaw MK, Ginger ML, Gaskell SJ, McKean PG, Gull K** (2006) Flagellar motility is required for the viability of the bloodstream trypanosome. *Nature* **440**:224–227
- Brun R, Schönenberger M** (1979) Cultivation and in vitro cloning or procyclic culture forms of *Trypanosoma brucei* in a semi-defined medium. Short communication. *Acta Trop* **36**:289–292
- Casey DM, Inaba K, Pazour GJ, Takada S, Wakabayashi K, Wilkerson CG, Kamiya R, Witman GB** (2003) DC3, the 21-kDa subunit of the outer dynein arm-docking complex (ODA-DC), is a novel EF-hand protein important for assembly of both the outer arm and the ODA-DC. *Mol Biol Cell* **14**:3650–3663
- Chin D, Means AR** (2000) Calmodulin: a prototypical calcium sensor. *Trends Cell Biol* **10**:322–328
- Davidge JA, Chambers E, Dickinson HA, Towers K, Ginger ML, McKean PG, Gull K** (2006) Trypanosome IFT mutants provide insight into the motor location for mobility of the flagella connector and flagellar membrane formation. *J Cell Sci* **119**:3935–3943
- Demonchy R, Blisnick T, Deprez C, Toutirais G, Lousert C, Marande W, Grellier P, Bastin P, Kohl L** (2009) Kinesin 9 family members perform separate functions in the trypanosome flagellum. *J Cell Biol* **187**:615–622
- DiPetrillo CG, Smith EF** (2010) Pcdp1 is a central apparatus protein that binds Ca²⁺-calmodulin and regulates ciliary motility. *J Cell Biol* **189**:601–612
- Dymek EE, Smith EF** (2007) A conserved CaM- and radial spoke associated complex mediates regulation of flagellar dynein activity. *J Cell Biol* **179**:515–526
- Eid JE, Sollner-Webb B** (1991) Homologous recombination in the tandem calmodulin genes of *Trypanosoma brucei* yields multiple products: compensation for deleterious deletions by gene amplification. *Genes Dev* **5**:2024–2032
- Gadelha C, Wickstead B, de Souza W, Gull K, Cunha-e-Silva N** (2005) Cryptic paraflagellar rod in endosymbiont-containing kinetoplastid protozoa. *Eukaryot Cell* **4**:516–525
- Gadelha C, Wickstead B, Gull K** (2007) Flagellar and ciliary beating in trypanosome motility. *Cytoskeleton* **64**:629–643
- Ginger ML, Portman N, McKean PG** (2008) Swimming with protists: perception, motility and flagellum assembly. *Nature Rev Microbiol* **6**:838–850
- Griffiths S, Portman N, Taylor PR, Gordon S, Ginger ML, Gull K** (2007) RNAi mutant induction in vivo demonstrates the essential nature of trypanosome flagellar function during mammalian infection. *Eukaryot Cell* **6**:148–1250
- Holwill ME, McGregor JL** (1976) Effects of calcium on flagellar movement in the trypanosome *Crithidia oncopelti*. *J Exp Biol* **65**:229–242
- Höög JL, Bouchet-Marquis C, McIntosh JR, Hoenger A, Gull K** (2012) Cryo-electron tomography and 3-D analysis of the intact flagellum in *Trypanosoma brucei*. *J Struct Biol* **178**:189–198
- Hughes LC, Ralston KS, Hill KL, Zhou ZH** (2012) Three-dimensional structure of the trypanosome flagellum suggests that the paraflagellar rod functions as a biomechanical spring. *Plos One* **7**:e25700
- Hunger-Glaser I, Seebeck T** (1997) Deletion of the genes for the paraflagellar rod protein PFR-A in *Trypanosoma brucei* is probably lethal. *Mol Biochem Parasitol* **90**:347–351
- Kohl L, Sherwin T, Gull K** (1999) Assembly of the paraflagellar rod and the flagellum attachment zone complex during the *Trypanosoma brucei* cell cycle. *J Eukaryot Microbiol* **46**:105–109
- Koyfman AY, Schmid MF, Gheiratmand L, Fu CJ, Khant HA, Huang D, He CY, Chiu W** (2011) Structure of *Trypanosoma brucei* flagellum accounts for its bihelical motion. *Proc Natl Acad Sci USA* **108**:11105–11108
- Lacomble S, Portman N, Gull K** (2009) A protein-protein interaction map of the *Trypanosoma brucei* paraflagellar rod. *PLoS One* **4**:e7685
- LaCount DJ, Barrett B, Donelson JE** (2002) *Trypanosoma brucei* FLA1 is required for flagellum attachment and cytokinesis. *J Biol Chem* **277**:17580–17588
- Lye L-F, Owens K, Shi H, Murta SMF, Vieira AC, Turco SJ, Tschudi C, Ullu E, Beverley SM** (2010) Retention and Loss of RNA interference pathways in trypanosomatid protozoans. *PLoS Pathogens* **6**:e1001161
- Maga JA, Sherwin T, Francis S, Gull K, LeBowitz JH** (1999) Genetic dissection of the *Leishmania* paraflagellar rod, a unique flagellar cytoskeleton structure. *J Cell Sci* **112**:2753–2763
- McCulloch R, Vassella E, Burton P, Boshart M, Barry JD** (2004) Transformation of monomorphic and pleomorphic *Trypanosoma brucei*. *Methods Mol Biol* **262**:53–86
- Moreira-Leite FF** (2002) PhD thesis, University of Manchester, UK
- Moreira-Leite FF, Sherwin T, Kohl L, Gull K** (2001) A trypanosome structure involved in transmitting cytoplasmic information during cell division. *Science* **294**:610–612
- Nozaki T, Haynes PA, Cross GA** (1996) Characterization of the *Trypanosoma brucei* homologue of a *Trypanosoma cruzi* flagellum-adhesion glycoprotein. *Mol Biochem Parasitol* **82**:245–255
- Oberholzer M, Marti G, Baresic M, Kunz S, Hemphill A, Seebeck T** (2007) The *Trypanosoma brucei* cAMP phosphodiesterases TbPDEB1 and TbPDEB2: flagellar enzymes that are essential for parasite virulence. *FASEB J* **21**:720–731
- Ploubidou A, Robinson DR, Docherty RC, Ogbadoyi EO, Gull K** (1999) Evidence for novel cell cycle checkpoints in trypanosomes: kinetoplast segregation and cytokinesis in the absence of mitosis. *J Cell Sci* **112**:4641–4650
- Poon SK, Peacock L, Gibson W, Gull K, Kelly S** (2012) A modular and optimised single marker system for generating *Trypanosoma brucei* cell lines expressing T7 RNA polymerase and the tetracycline repressor. *Open Biol* **2**:120033
- Portman N, Gull K** (2010) The paraflagellar rod of kinetoplastid parasites: from structure to components and function. *Int J Parasitol* **40**:135–148
- Portman N, Lacomble S, Thomas B, McKean PG, Gull K** (2009) Combining RNA interference mutants and comparative

proteomics to identify protein components and dependences in a eukaryotic flagellum. *J Biol Chem* **284**:5610–5619

Pullen TJ, Ginger ML, Gaskell SJ, Gull K (2004) Protein targeting of an unusual, evolutionarily conserved adenylate kinase to a eukaryotic flagellum. *Mol Biol Cell* **15**:3257–3265

Ralston KS, Lerner AG, Diener DR, Hill KL (2006) Flagellar motility contributes to cytokinesis in *Trypanosoma brucei* and is modulated by an evolutionarily conserved dynein regulatory system. *Eukaryot Cell* **5**:696–711

Ridgley E, Webster P, Patton C, Ruben L (2000) Calmodulin-binding properties of the paraflagellar rod complex from *Trypanosoma brucei*. *Mol Biochem Parasitol* **109**:195–201

Robinson DR, Sherwin T, Ploubidou A, Byard EH, Gull K (1995) Microtubule polarity and dynamics in the control of organelle positioning, segregation, and cytokinesis in the trypanosome cell cycle. *J Cell Biol* **128**:1163–1172

Rusconi F, Durand-Dubief M, Bastin P (2005) Functional complementation of RNA interference mutants in trypanosomes. *BMC Biotechnol* **5**:6

Santrich C, Moore L, Sherwin T, Bastin P, Brokaw C, Gull K, LeBowitz JH (1997) A motility function for the paraflagellar rod of *Leishmania* parasites revealed by PFR-2 gene knockouts. *Mol Biochem Parasitol* **90**:95–109

Sherwin T, Gull K (1989) The cell division cycle of *Trypanosoma brucei brucei*: timing of event markers and cytoskeletal modulations. *Philos Trans R Soc Lond B Biol Sci* **323**:573–588

Smith EF (2002) Regulation of flagellar dynein by calcium and a role for an axonemal calmodulin and calmodulin-dependent kinase. *Mol Biol Cell* **13**:3303–3313

Sun Y, Wang C, Yuan YA, He CY (2013) An intra-cellular membrane junction mediated by flagellum adhesion glycoproteins links flagellum biogenesis to cell morphogenesis in *Trypanosoma brucei*. *J Cell Sci* **126**:520–531

Turnock DC, Izquierdo L, Ferguson MA (2007) The de novo synthesis of GDP-fucose is essential for flagellar adhesion and cell growth in *Trypanosoma brucei*. *J Biol Chem* **282**:28853–28863

Vaughan S (2010) Assembly of the flagellum and its role in cell morphogenesis in *Trypanosoma brucei*. *Curr Opin Microbiol* **13**:453–458

Vaughan S, Kohl L, Ngai I, Wheeler RJ, Gull K (2008) A repetitive protein essential for the flagellum attachment zone filament structure and function in *Trypanosoma brucei*. *Protist* **159**:127–136

Vickerman K (1969) On the surface coat and flagellar adhesion in trypanosomes. *J Cell Sci* **5**:163–193

Wang Z, Morris JC, Drew ME, Englund PT (2000) Inhibition of *Trypanosoma brucei* gene expression by RNAi interference using an integratable vector with opposing T7 promoters. *J Biol Chem* **275**:40174–40179

Wickstead B, Ersfeld K, Gull K (2002) Targeting of a tetracycline-inducible expression system to the transcriptionally silent minichromosomes of *Trypanosoma brucei*. *Mol Biochem Parasitol* **125**:211–216

Wirtz E, Leal S, Ochatt C, Cross GA (1999) A tightly regulated inducible expression system for conditional gene knock-outs and dominant-negative genetics in *Trypanosoma brucei*. *Mol Biochem Parasitol* **99**:89–101

Yang P, Yang C, Sale WS (2004) Flagellar radial spoke protein 2 is a calmodulin binding protein required for motility in *Chlamydomonas reinhardtii*. *Eukaryot Cell* **3**:72–81

Yang P, Diener DR, Rosenbaum JL, Sale WS (2001) Localization of calmodulin and dynein light chain LC8 in flagellar radial spokes. *J Cell Biol* **153**:1315–1326

Zhou Q, Liu B, Sun Y, He CY (2011) A coiled-coil- and C2-domain-containing protein is required for FAZ assembly and cell morphology in *Trypanosoma brucei*. *J Cell Sci* **124**:3848–3858

Available online at www.sciencedirect.com

SciVerse ScienceDirect